

# Precision Measurements of Light Quenching in $\text{CaWO}_4$ Crystals at mK Temperatures

R. Strauss,<sup>1,2,\*</sup> G. Angloher,<sup>2</sup> A. Bento,<sup>3</sup> C. Bucci,<sup>4</sup> L. Canonica,<sup>4</sup> A. Erb,<sup>1,5</sup> F.v. Feilitzsch,<sup>1</sup> P. Gorla,<sup>4</sup>  
 A. Gütlein,<sup>1</sup> D. Hauff,<sup>2</sup> J. Jochum,<sup>6</sup> H. Kraus,<sup>7</sup> J.-C. Lanfranchi,<sup>1</sup> J. Loebell,<sup>6</sup> A. Münster,<sup>1</sup> F. Petricca,<sup>2</sup>  
 W. Potzel,<sup>1</sup> F. Pröbst,<sup>2</sup> F. Reindl,<sup>2</sup> S. Roth,<sup>1</sup> K. Rottler,<sup>6</sup> C. Sailer,<sup>6</sup> K. Schäffner,<sup>4</sup> J. Schieck,<sup>8</sup>  
 S. Scholl,<sup>6</sup> S. Schönert,<sup>1</sup> W. Seidel,<sup>2</sup> M.v. Sivers,<sup>1</sup> L. Stodolsky,<sup>2</sup> C. Strandhagen,<sup>6</sup> A. Tanzke,<sup>2</sup>  
 M. Uffinger,<sup>6</sup> A. Ulrich,<sup>1</sup> I. Usherov,<sup>6</sup> S. Wawoczny,<sup>1</sup> M. Willers,<sup>1</sup> M. Wüstrich,<sup>1</sup> and A. Zöller<sup>1</sup>

(The CRESST Collaboration)

W. Carli,<sup>9</sup> C. Ciemniak,<sup>1</sup> H. Hagn,<sup>1</sup> and D. Hellgartner<sup>1</sup>

<sup>1</sup>*Physik-Department, Technische Universität München, D-85748 Garching, Germany*

<sup>2</sup>*Max-Planck-Institut für Physik, D-80805 München, Germany*

<sup>3</sup>*CIUC, Departamento de Física, Universidade de Coimbra, P3004 516 Coimbra, Portugal*

<sup>4</sup>*INFN, Laboratori Nazionali del Gran Sasso, I-67010 Assergi, Italy*

<sup>5</sup>*Walther-Meißner-Institut für Tieftemperaturforschung, D-85748 Garching, Germany*

<sup>6</sup>*Physikalisches Institut, Eberhard-Karls-Universität Tübingen, D-72076 Tübingen, Germany*

<sup>7</sup>*Department of Physics, University of Oxford, Oxford OX1 3RH, United Kingdom*

<sup>8</sup>*Institut für Hochenergiephysik der Österreichischen Akademie der Wissenschaften, A-1050 Wien, Austria*

<sup>9</sup>*Maier-Leibnitz-Laboratorium, Ludwig-Maximilians-Universität München, D-85748 Garching, Germany*

(Dated: January 16, 2014)

Scintillating  $\text{CaWO}_4$  single crystals are a promising multi-element target for rare-event searches and are currently used in the direct Dark Matter experiment CRESST (Cryogenic Rare Event Search with Superconducting Thermometers). The relative light output of different particle interactions in  $\text{CaWO}_4$  is quantified by Quenching Factors (QFs). These are essential for an active background discrimination and the identification of a possible signal induced by weakly interacting massive particles (WIMPs). We present the first precise measurements of the QFs of O, Ca and W at mK temperatures by irradiating a cryogenic detector with a fast neutron beam. A clear energy dependence of the QFs and a variation between different  $\text{CaWO}_4$  single crystals were observed for the first time. For typical CRESST detectors the QFs in the region-of-interest (10-40 keV) are  $QF_O^{ROI} = (11.2 \pm 0.5)\%$ ,  $QF_{Ca}^{ROI} = (5.94 \pm 0.49)\%$  and  $QF_W^{ROI} = (1.72 \pm 0.21)\%$ . The latest CRESST data (run32) is reanalyzed using these fundamentally new results on light quenching in  $\text{CaWO}_4$  having moderate influence on the WIMP analysis. Their relevance for future CRESST runs and for the clarification of previously published results of direct Dark Matter experiments is emphasized.

Rare-event searches for Dark Matter (DM) in the form of weakly interacting massive particles (WIMPs) [1, 2] have reached impressive sensitivities during the last decade [3]. Well motivated WIMP candidates with masses  $m_\chi$  between a few  $\text{GeV}/c^2$  and a few  $\text{TeV}/c^2$  might be detectable via nuclear recoils of few keV in terrestrial experiments [4]. While the DAMA/LIBRA [5], and recently the CoGeNT [6], CRESST [7], and the CDMS(Si) [8] experiments observed excess signals that might be interpreted as induced by DM particles with  $m_\chi \sim 10 \text{ GeV}/c^2$  at WIMP-nucleon cross-sections of  $\sim 10^{-4} \text{ pb}$ , this scenario is ruled out by the LUX [9] and XENON100 [10] experiments, and almost excluded by the CDMS(Ge) [11, 12] and EDELWEISS [13, 14] experiments. It is strongly disfavoured by accelerator constraints [15, 16] and in mild tension with an extended analysis [17] of published CRESST data [18].

The CRESST experiment [7] employs scintillating  $\text{CaWO}_4$  crystals [19, 20] as a multi-element target material. The key feature of a CRESST detector module is the simultaneous measurement of the recoil energy  $E_r$  by a particle interaction in the crystal (operated as cryogenic calorimeter at mK temperatures [21])

and the corresponding scintillation-light energy  $E_l$  by a separate cryogenic light absorber. Since the relative light yield  $LY = E_l/E_r$  is reduced for highly ionizing particles compared to electron recoils (commonly referred to as quenching) nuclear-recoil events can be discriminated from  $e^-/\gamma$  and  $\alpha$  backgrounds. The phenomenological Birks model [22] predicts this quenching effect to be stronger the higher the mass number  $A$  of the recoiling ion, which allows to distinguish, in general, between O ( $A \approx 16$ ), Ca ( $A \approx 40$ ) and W ( $A \approx 184$ ) recoils. The expected WIMP-recoil spectrum - assuming coherent scattering - is completely dominated by W-scatters for  $m_\chi \gtrsim 20 \text{ GeV}/c^2$ . However, the light targets O and Ca make CRESST detectors particularly sensitive to low-mass WIMPs of  $1 \text{ GeV} \lesssim m_\chi \lesssim 20 \text{ GeV}$ . Furthermore, the knowledge of the recoil composition of O, Ca and W allows a test of the assumed  $A^2$ -dependence of the spin-independent WIMP-nucleon cross-section [2]. In addition, background neutrons, which are mainly visible as O-scatters (from kinematics [23]), can be discriminated statistically.

The mean LY of  $e^-/\gamma$  events ( $LY_\gamma$ ) is energy dependent and phenomenologically parametrized as

$LY_\gamma(E_r) = (p_0 + p_1 E_r)(1 - p_2 \exp(-E_r/p_3))$  [24]. By convention,  $LY_\gamma(122 \text{ keV})$  is normalized to unity. The parameters  $p_0$ ,  $p_1$ ,  $p_2$  and  $p_3$  are derived from a maximum-likelihood (ML) fit for every detector module individually. For the module used in this work the fit yields:  $p_0 = 1.07$ ,  $p_1 = -1.40 \cdot 10^{-5} \text{ keV}^{-1}$ ,  $p_2 = 6.94 \cdot 10^{-2}$  and  $p_3 = 147 \text{ keV}$  (errors are negligible for the following analysis). The exponential decrease towards lower recoil energies (quantified by  $p_2$  and  $p_3$ ) accounts for the scintillator non-proportionality [25]. The Quenching Factor (QF) of a nucleus  $x$  - in general energy dependent - is defined as  $QF_x(E_r) = LY_x(E_r)/LY_{\gamma,corr}(E_r)$  where  $LY_x$  is the mean LY of a nuclear recoil  $x$ . For normalization, the LY of  $e^-/\gamma$  events corrected for the scintillator non-proportionality (which is not observed for nuclear recoils) is used by convention:  $LY_{\gamma,corr} = p_0 + p_1 E_r$ . For typical CRESST detector modules, the uncertainties in energy and LY are well described by gaussians [7] consistent with photon-counting statistics in the energy range considered in this work.

Since the resolution of light-detectors operated in the CRESST setup at present is not sufficient to disentangle O, Ca and W recoils unambiguously, dedicated experiments to measure the QFs of  $\text{CaWO}_4$  are necessary. Earlier attempts yield inconclusive results, in particular for the value of  $QF_W$  [26–28].

At the accelerator of the Maier-Leibnitz-Laboratorium (MLL) in Garching a dedicated neutron-scattering facility for precision measurements of QFs at mK temperatures was set up (see FIG. 1). A pulsed  $^{11}\text{B}$  beam of  $\sim 65 \text{ MeV}$  in bunches of 2-3 ns (FWHM) produces monoenergetic neutrons of  $\sim 11 \text{ MeV}$  via the nuclear reaction  $p(^{11}\text{B},n)^{11}\text{C}$  in a pressurized  $\text{H}_2$  target [29]. These neutrons are irradiated onto a CRESST-like detector module consisting of a  $\sim 10 \text{ g}$  cylindrical  $\text{CaWO}_4$  single crystal (20 mm in diameter, 5 mm in height) and a separated Si light absorber (20 mm in diameter,  $500 \mu\text{m}$  thick) [30]. Both are operated as cryogenic detectors in a dilution refrigerator at  $\sim 20 \text{ mK}$  [31]. Undergoing elastic (single) nuclear scattering in  $\text{CaWO}_4$  the neutrons are tagged at a fixed scattering angle  $\Theta$  in an array of 40 liquid-scintillator (EJ301) detectors which allow fast timing ( $\sim 2 \text{ ns}$ ) and  $n/\gamma$  discrimination. Depending upon which of the three nuclei is hit a distinct amount of energy is deposited by the neutron in the crystal. Triple-coincidences between (1) a  $^{11}\text{B}$  pulse on the  $\text{H}_2$  target, (2) a neutron pulse in a liquid-scintillator detector and (3) a nuclear-recoil event in the  $\text{CaWO}_4$  crystal can be extracted from the data set. A neutron time-of-flight (TOF) measurement between neutron production and detection combined with a precise phononic measurement of the energy deposition in the crystal (resolution  $\sim 1 \text{ keV}$  (FWHM)) allows an identification of the recoiling nucleus. To derive the individual QF the corresponding scintillation-light output is measured simultaneously by the light detector. Since the onset uncertainty of cryodetector pulses is large

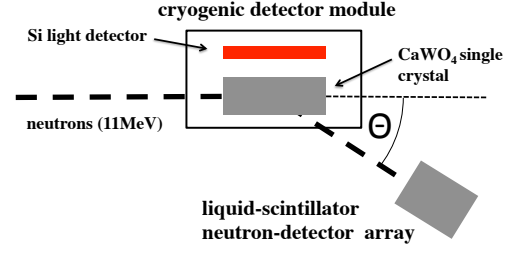


FIG. 1. Schematic experimental setup of the neutron-scattering facility. Neutrons produced by the accelerator are scattered off a CRESST-like detector module (operated at 20 mK) and tagged in liquid-scintillator neutron detectors at a fixed scattering angle  $\Theta$ .

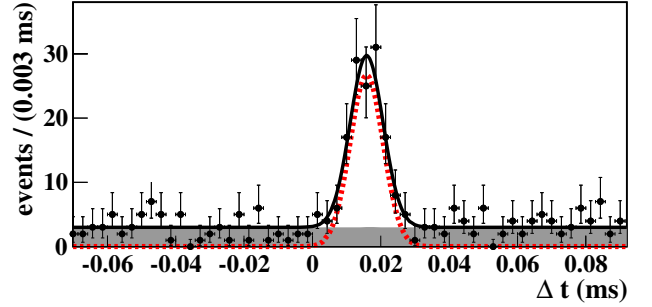


FIG. 2. Histogram of the time difference  $\Delta t$  between neutron events with the correct TOF and the closest W-recoil in the  $\text{CaWO}_4$  crystal ( $E_r = 100 \pm 20 \text{ keV}$ ). A fit to the distribution (solid black line) including a constant for the accidental background (shaded area) and a gaussian for the triple-coincidences on W (dashed red line) is shown. 158 W-scatters are identified with a signal-to-background ratio of  $\sim 7 : 1$ .

( $\sim 5 \mu\text{s}$ ) compared to typical neutron TOFs ( $\sim 50 \text{ ns}$ ) an offline coincidence analysis has to be performed [24].

The experiment was optimized for the measurement of  $QF_W$  [24, 32]. To enhance the number of W-scatters a scattering angle of  $\Theta = 80^\circ$  was chosen due to scattering kinematics [26]. For this specific angle, the expected recoil energy of triple-coincident events is  $\sim 100 \text{ keV}$  for W,  $\sim 450 \text{ keV}$  for Ca, and  $\sim 1.1 \text{ MeV}$  for O. In  $\sim 3$  weeks of beam time a total of  $\sim 10^8$  cryodetector pulses were recorded. FIG. 2 shows the time difference  $\Delta t$  between neutron events with the correct TOF identified in one of the liquid-scintillator detectors and the closest W-recoil (in time) in the  $\text{CaWO}_4$  crystal ( $E_r = 100 \pm 20 \text{ keV}$ ). A gaussian peak of triple-coincidences on W (dashed red line) at  $\Delta t \approx 0.016 \text{ ms}$  and a width of  $\sigma_t \approx 4.8 \mu\text{s}$  (onset resolution of the cryodetector) is observed above a background due to accidental coincidences uniformly distributed in time (shaded area). Within the  $2\sigma$ -bounds of the peak 158 W-scatters are identified with a signal-to-background (S/B) ratio of  $\sim 7 : 1$ .

The mean LY of the extracted W-scatters is found at a lower value compared to the mean LY of all nu-

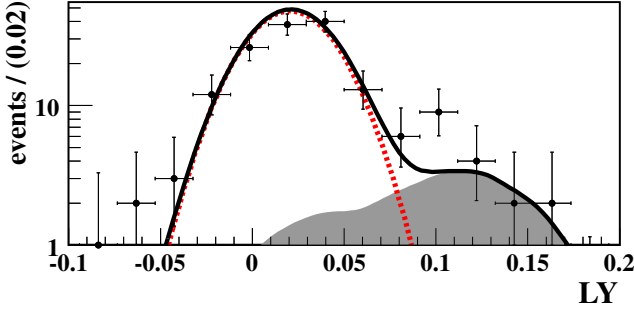


FIG. 3. LY histogram of the 158 events identified as triple-coincidences on W. A fit to the distribution (solid black line) is shown which includes a gaussian (dashed red line) accounting for W-scatters and the background-pdf (shaded area) describing accidental coincidences. The simultaneous ML fit including the timing distribution yields  $QF_W = (1.96 \pm 0.22)\%$ .

clear recoils, i.e., the (overlapping) contributions of O, Ca and W if no coincidence measurement is involved. The accidental coincidences have a LY-distribution equal to that which is modelled by a probability-density function (background-pdf) [24]. A simultaneous maximum-likelihood (ML) fit is performed including (1) the timing distribution which fixes the S/B ratio and the number of identified W-events, and (2) the LY distribution described by a gaussian (W-events) and the background-pdf. The final results are  $LY_W = 0.0208 \pm 0.0024$  and  $QF_W = (1.96 \pm 0.22)\%$ , correspondingly (errors are dominated by statistics). FIG. 3 shows the LY histogram of the identified events and the fit by the gaussian (dashed red line) and the background-pdf (shaded area).

For the measurement of  $QF_{Ca}$  and  $QF_O$  no coincidence signals are necessary, instead, an analysis of the nuclear-recoil data alone is sufficient. Commonly CRESST data is displayed in the energy-LY plane [7] giving rise to nearly horizontal bands which correspond to different types of particle interactions ( $LY \approx 1$  for electron and  $LY \lesssim 0.2$  for nuclear recoils). The nuclear-recoil bands of the data recorded during  $\sim 1$  week of beam time ( $\sim 5 \cdot 10^5$  pulses) are shown in FIG. 4 bottom (grey dots). From kinematics using  $\sim 11$  MeV neutrons as probes the O-recoil band extends up to  $\sim 2.4$  MeV while the Ca- and W-bands extend up to  $\sim 1.05$  MeV and  $\sim 240$  keV, respectively [29]. Despite the strong overlap of the 3 nuclear-recoil bands the contributions of O and Ca fitted by two gaussians can be disentangled at  $E_r \gtrsim 350$  keV (see FIG. 4 top) due to high statistics and a good light-detector resolution. In FIG. 5 the results for  $QF_O$  and  $QF_{Ca}$  (red error bars) derived by these independent one-dimensional (1-dim) fits are shown for selected recoil-energy slices of 20 keV in width. All parameters in the fit are left free except for the LY-resolutions which are fixed by a ML fit of the electron-recoil band [24]. While  $QF_O$  clearly rises towards lower recoil energies, this effect is less pro-

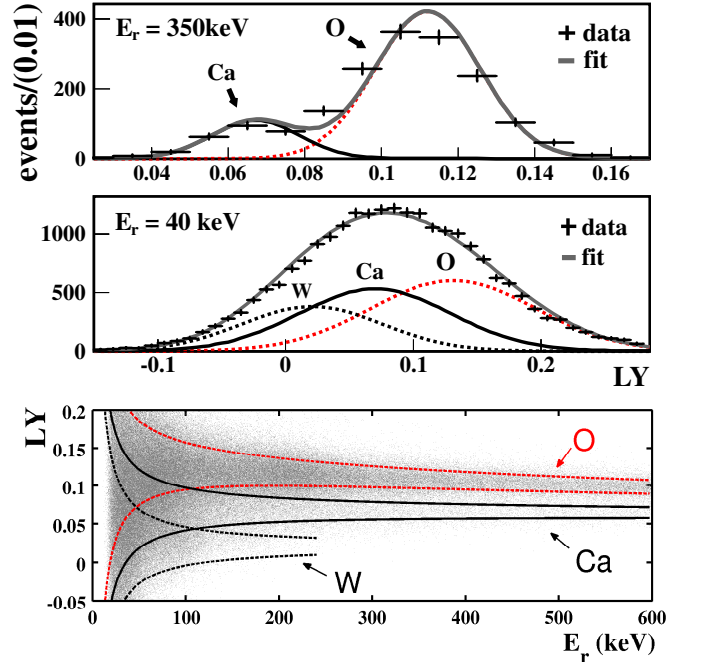


FIG. 4. Top/Middle: LY histograms of two energy slices at 350 and 40 keV (of 20 keV in width) fitted by gaussians. Bottom: Neutron-induced nuclear-recoil events of O, Ca, and W plotted in the LY-energy plane (grey dots). The corresponding  $1\sigma$  acceptance bounds as derived from the correlated ML fit are indicated (see text).

nounced for  $QF_{Ca}$ .

Below  $\sim 350$  keV, due to the strong overlap of the nuclear-recoil bands, this simple approach fails. Instead, a correlated ML fit was performed based on the following assumptions: (1) for the mean LY of O- and Ca-scatters the phenomenological parametrization  $LY_x(E_r) = LY_x^\infty (1 + f_x \cdot \exp(-E_r/\lambda_x))$  is proposed with the free parameters  $LY_x^\infty$  (LY at  $E_r = \infty$ ),  $f_x$  (fraction of energy-dependent component) and  $\lambda_x$  (exponential decay with energy), and (2) the mean LY of W-scatters is approximated to be constant in the relevant energy range (up to  $\sim 240$  keV) at the value precisely measured with the triple-coincidence technique ( $LY_W = 0.0208 \pm 0.0024$ ). These assumptions are supported by the result of the 1-dim fits (see FIG. 5), by Birks' model [22], and by a recent work [33] which predict the strength of the energy-dependence to decrease with A. The nuclear-recoil bands are cut into energy intervals of 10 keV (20 keV to 1 MeV), of 20 keV (1 MeV to 1.4 MeV) and 50 keV (above 1.4 MeV) and fitted with up to 3 gaussians depending on the recoil energy (e.g., shown in FIG. 4 middle for  $E_r = 40$  keV). Except for the assumptions mentioned above and the LY-resolution all parameters are left free in the fit. The fit converges over the entire energy range (20-1800 keV). In TABLE I the results for  $LY_x^\infty$ ,  $f_x$  and  $\lambda_x$  are presented which correspond, e.g. at 40 keV, to  $QF_O = (12.6 \pm 0.5)\%$ ,

TABLE I. Results for the free parameters  $LY_x^\infty$ ,  $f_x$  and  $\lambda_x$  of the ML analysis. The statistical errors are given at  $1\sigma$  C.L.

nucleus	$LY_x^\infty$	$f_x$	$\lambda_x$
O	$0.07908 \pm 0.00002$	$0.7088 \pm 0.0008$	$567.1 \pm 0.9$
Ca	$0.05949 \pm 0.00078$	$0.1887 \pm 0.0022$	$801.3 \pm 18.8$

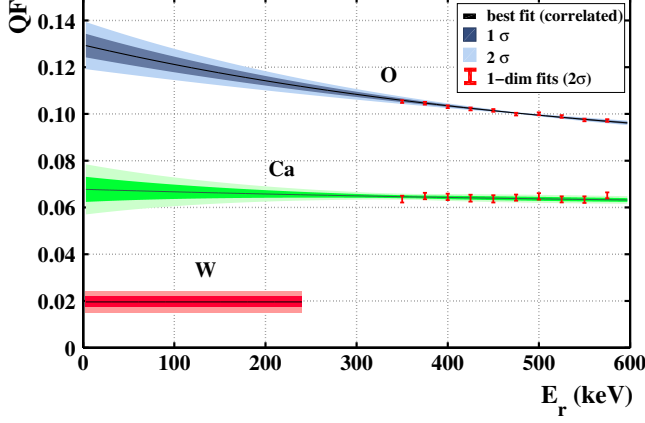


FIG. 5. Results of the correlated ML analysis for  $QF_O$ ,  $QF_{Ca}$  and  $QF_W$  (solid lines). The shaded areas indicate the  $1\sigma$  and  $2\sigma$  bounds. For the first time a clear energy dependence of  $QF_O$  and  $QF_{Ca}$  is observed. These results are in agreement with that of the 1-dim fits of discrete energy intervals (see text) shown as red error bars.  $QF_W$  is fixed (in the correlated fit) at the value measured by the triple-coincidence technique.

$QF_{Ca} = (6.73 \pm 0.43)\%$  (here, the errors are dominated by systematics) and  $QF_W = (1.96 \pm 0.22)\%$  at  $1\sigma$  C.L. The  $1\sigma$  acceptance bounds of O, Ca and W recoils as obtained in the correlated ML fit are shown in FIG. 4 bottom. The final results for  $QF_O$ ,  $QF_{Ca}$  and  $QF_W$  are presented in FIG. 5 and are found to be in perfect agreement with the outcome of the 1-dim fits (red error bars). These are the first experimental results which clearly show a rise of the QFs of O (Ca) of  $\sim 28\%$  ( $\sim 6\%$ ) towards the ROI (10-40 keV) compared to that at a recoil energy of 500 keV.

In previous works, the QFs of  $\text{CaWO}_4$  were assumed to be constant over the entire energy range [7]. A statistical analysis shows that this simple model is clearly disfavoured. Employing a likelihood-ratio test in combination with Monte-Carlo simulations gives a p-value of  $p < 10^{-5}$  for the data presented here to be consistent with constant QFs. Furthermore, the derived energy spectra of the individual recoiling nuclei agree with the expectation from incident 11 MeV neutrons while the constant QF approach provides non-physical results.

In the present paper, using the 8 detector modules operated in the last CRESST measurement campaign (run32) an additional aspect was investigated: the variation of the quenching behaviour among *different*  $\text{CaWO}_4$  crystals [24]. Nuclear recoils acquired during neutron-

TABLE II. QF results averaged over the ROI (10-40 keV) and adjusted by the scaling factor  $\epsilon$  for the modules Rita and Daisy, and the mean ( $\emptyset$ ) of all run32 detectors ( $1\sigma$  errors).

	$\epsilon$	$QF_O^{\text{ROI}}[\%]$	$QF_{Ca}^{\text{ROI}}[\%]$	$QF_W^{\text{ROI}}[\%]$
Rita	$0.844 \pm 0.006$	$10.8 \pm 0.5$	$5.70 \pm 0.44$	$1.65 \pm 0.19$
Daisy	$0.939 \pm 0.021$	$12.0 \pm 0.7$	$6.33 \pm 0.58$	$1.84 \pm 0.24$
$\emptyset$	$0.880 \pm 0.011$	$11.2 \pm 0.5$	$5.94 \pm 0.49$	$1.72 \pm 0.21$

calibration campaigns of CRESST run32 are completely dominated by O-scatters at  $E_r \gtrsim 150$  keV (from kinematics) [7]. Despite low statistics (a factor of  $\sim 100$  less compared to the measurement presented here) in the available data, the mean LY of O-events can be determined by a gaussian fit with a precision of  $\mathcal{O}(1\%)$  for every module. In this way, the mean QF of O between 150 and 200 keV was determined individually for the 8 detector modules operated in run32 ( $\overline{QF_O^*}$ ) and for the reference detector operated at the neutron-scattering facility ( $\overline{QF_O}$ ). Different values of  $\overline{QF_O^*}$  are observed for the CRESST detector crystals (variation by  $\sim 11\%$ ) and for the reference crystal ( $\sim 12\%$  higher than the mean of  $\overline{QF_O^*}$ ). This variation appears to be correlated with the crystal's optical quality. The QF - which is a relative quantity - is found to be lower if a crystal has a smaller defect density and thus a higher absolute light output, i.e., the LY of nuclear recoils is less affected by an increased defect density. This is in agreement with the prediction described in a recent work [33]. In the present paper, a simple model to account for this variation is proposed: For every detector module which is to be calibrated a scaling factor  $\epsilon$  is introduced,  $\epsilon = \overline{QF_O^*} / \overline{QF_O}$ . Then, within this model the QFs of the nucleus  $x$  can be calculated for every module by  $QF_x^*(E_r) = \epsilon \cdot QF_x(E_r)$  where  $QF_x$  is the value precisely measured within this work. The nuclear-recoil behaviour of CRESST modules is well described by energy-dependent QFs. In TABLE II the QFs, averaged over the ROI (10-40 keV), and the scaling factor  $\epsilon$  are listed for two selected detector modules (Rita and Daisy, with the lowest and highest absolute light output, respectively) and the mean of all 8 detector modules of run32 ( $\emptyset$ ),  $QF_O^{\text{ROI}} = (11.2 \pm 0.5)\%$ ,  $QF_{Ca}^{\text{ROI}} = (5.94 \pm 0.49)\%$  and  $QF_W^{\text{ROI}} = (1.72 \pm 0.21)\%$ .

We now turn to the effect of energy-dependent quenching since constant QFs as assumed in earlier CRESST publications do not sufficiently describe the behaviour of the nuclear-recoil bands. The value of  $QF_O$  in the ROI was underestimated by  $\sim 8\%$  while the room-temperature measurements overestimated the values of  $QF_{Ca}$  and  $QF_W$  by  $\sim 7\%$  and  $\sim 130\%$ , respectively [7]. Therefore, the parameter space of accepted nuclear recoils is larger than assumed in earlier publications (by  $\sim 46\%$ ) requiring a re-analysis of the published CRESST data.

During the latest measuring campaign (run32) a statisti-

cally significant signal ( $4.2\sigma$ ) above known backgrounds was observed. If interpreted as induced by DM particles two WIMP solutions were found [7], e.g. at a mass of  $m_\chi = 11.6 \text{ GeV}/c^2$  with a WIMP-nucleon cross section of  $\sigma_\chi = 3.7 \cdot 10^{-5} \text{ pb}$ . The dedicated ML analysis was repeated using the new QF values ( $\emptyset$  in TABLE II) yielding  $m_\chi = 12.0 \text{ GeV}/c^2$  and  $\sigma_\chi = 3.2 \cdot 10^{-5} \text{ pb}$  at  $3.9\sigma$ . Beside this moderate change of the WIMP parameters also the background composition ( $e^-$ ,  $\gamma$ , neutrons,  $\alpha$ 's and  $^{206}\text{Pb}$ ) is influenced. This is mainly due to the significantly lower value of  $QF_W$  which increases the leakage of  $^{206}\text{Pb}$  recoils into the ROI (by  $\sim 18\%$ ). The other WIMP solution is influenced similarly:  $m_\chi$  changes from  $25.3$  to  $25.5 \text{ GeV}/c^2$ ,  $\sigma_\chi$  from  $1.6 \cdot 10^{-6}$  to  $1.5 \cdot 10^{-6} \text{ pb}$  and the significance drops slightly from  $4.7$  to  $4.3\sigma$ .

In conclusion, the first precise measurement of  $QF_W$  at mK temperatures and under conditions comparable to that of the CRESST experiment was obtained at the neutron-scattering facility in Garching by an extensive triple-coincidence technique. Furthermore, the QFs of all three nuclei in  $\text{CaWO}_4$  were precisely determined by a dedicated maximum-likelihood analysis over the entire energy range ( $\sim 20$ – $1800 \text{ keV}$ ). The observed energy dependence of the QFs, which is more pronounced for lighter nuclei, has significant influence on the determination of the ROI for DM search with CRESST. The observed variation of the QFs between different  $\text{CaWO}_4$  crystals is related to the optical quality and can be adapted to every individual crystal by the simple model proposed above. The updated values of the QFs are highly relevant to disentangle the recoil composition (O, Ca and W) of a possible DM signal and, therefore, to determine the WIMP parameters. Since the separation between the O and W recoil bands is higher by  $\sim 46\%$  compared to earlier assumptions, background neutrons which are mainly visible as O-scatters [23] can be discriminated more efficiently from possible WIMP-induced events. A reanalysis of the run32 data shows a moderate influence of the new QF values on the WIMP parameters. The results obtained here are of importance for the current CRESST run (run33) and upcoming measuring campaigns. Providing a highly improved background level run33 has the potential to clarify the origin of the observed excess signal and to set competitive limits for the spin-independent WIMP-nucleon cross section in the near future. For the planned multi-material DM experiment EURECA (European Underground Rare Event Calorimeter Array) [34] the neutron-scattering facility will be an important tool to investigate the light quenching of alternative target materials in the future.

This research was supported by the DFG cluster of excellence: Origin and Structure of the Universe, the DFG Transregio 27: Neutrinos and Beyond, the Helmholtz Alliance for Astroparticle Physics, the Maier-Leibnitz-Laboratorium (Garching) and by the BMBF: Project

05A11WOC EURECA-XENON.

\* strauss@mpp.mpg.de

- [1] G. Bertone, D. Hooper, and J. Silk, *Phys.Rept.*, **405**, 279 (2005), arXiv:hep-ph/0404175 [hep-ph].
- [2] G. Jungman, M. Kamionkowski, and K. Griest, *Phys.Rept.*, **267**, 195 (1996), arXiv:hep-ph/9506380 [hep-ph].
- [3] P. Cushman *et al.*, (2013), arXiv:1310.8327 [hep-ex].
- [4] J. Lewin and P. Smith, *Astropart.Phys.*, **6**, 87 (1996).
- [5] R. Bernabei *et al.* (DAMA, LIBRA), *Eur.Phys.J.*, **C67**, 39 (2010), arXiv:1002.1028 [astro-ph.GA].
- [6] C. Aalseth *et al.* (CoGeNT), *Phys.Rev.Lett.*, **106**, 131301 (2011), arXiv:1002.4703 [astro-ph.CO].
- [7] G. Angloher *et al.* (CRESST), *Eur.Phys.J.*, **C72**, 1 (2012).
- [8] R. Agnese *et al.* (CDMS Collaboration), *Phys. Rev. Lett.*, **111**, 251301 (2013).
- [9] D. Akerib *et al.* (LUX Collaboration), (2013), arXiv:1310.8214 [astro-ph.CO].
- [10] E. Aprile *et al.* (XENON100), *Phys.Rev.Lett.*, **109**, 181301 (2012), arXiv:1207.5988 [astro-ph.CO].
- [11] Z. Ahmed *et al.* (CDMS-II), *Science*, **327**, 1619 (2010), arXiv:0912.3592 [astro-ph.CO].
- [12] Z. Ahmed *et al.* (CDMS-II), *Phys.Rev.Lett.*, **106**, 131302 (2011), arXiv:1011.2482 [astro-ph.CO].
- [13] E. Armengaud *et al.* (EDELWEISS), *Phys.Lett.*, **B702**, 329 (2011), arXiv:1103.4070 [astro-ph.CO].
- [14] E. Armengaud *et al.* (EDELWEISS), *Phys.Rev.*, **D86**, 051701 (2012), arXiv:1207.1815 [astro-ph.CO].
- [15] G. Aad *et al.* (ATLAS Collaboration), *JHEP*, **1304**, 075 (2013), arXiv:1210.4491 [hep-ex].
- [16] S. Chatrchyan *et al.* (CMS Collaboration), *JHEP*, **1209**, 094 (2012), arXiv:1206.5663 [hep-ex].
- [17] A. Brown, S. Henry, H. Kraus, and C. McCabe, *Phys. Rev. D*, **85**, 021301 (2012).
- [18] G. Angloher *et al.*, *Astropart.Phys.*, **31**, 270 (2009).
- [19] T. A. Edison, *Nature*, **53**, 470 (1896).
- [20] V. B. Mikhailik, H. Kraus, S. Henry, and A. J. B. Tolhurst, *Phys. Rev. B*, **75**, 184308 (2007).
- [21] F. Pröbst *et al.*, *J. Low Temp. Phys.*, **100**, 69 (1995).
- [22] J. Birks, *The Theory and Practice of Scintillation Counting* (Pergamon Press, 1964).
- [23] S. Scholl and J. Jochum, *J. Phys.:* Conference Series, **375**, 012020 (2012).
- [24] R. Strauss, Ph.D. thesis, TU München (2013).
- [25] R. Lang *et al.*, (2009), arXiv:0910.4414 [nucl-ex].
- [26] T. Jagemann *et al.*, *Astropart.Phys.*, **26**, 269 (2006).
- [27] J. Ninkovic *et al.*, *Nucl.Instrum.Meth.*, **A564**, 567 (2006), arXiv:astro-ph/0604094 [astro-ph].
- [28] I. Bavykina *et al.*, *Astropart.Phys.*, **28**, 489 (2007), arXiv:0707.0766 [physics.ins-det].
- [29] T. Jagemann, J. Jochum, and F. Feilitzsch, *Nucl.Instrum.Meth.*, **A551**, 245 (2005).
- [30] R. Strauss *et al.*, *J. Low Temp. Phys.*, **167**, 1063 (2012).
- [31] J.-C. Lanfranchi *et al.*, *Opt. Mat.*, **31**, 1405 (2009).
- [32] R. Strauss *et al.*, *J. Low Temp. Phys.*, accepted for publication.
- [33] S. Roth, Ph.D. thesis, TU München (2013).
- [34] H. Kraus *et al.*, *PoS, IDM2010*, 109 (2011).